A Robust Orientation System for Inclinometer With Full-Redundancy in Heavy Industry

A Robust Orientation System for Inclinometer with Full-Redundancy in Heavy Industry

Minh Long Hoang, *Member, IEEE*, Antonio Pietrosanto, *Senior Member, IEEE*

***Abstract*— In the heavy industry, high-quality inclinometer has been required in terms of accuracy, stability, and safety function for durable use in harsh environments. This paper proposes a robust orientation system for industrial inclinometer based on Microelectromechanical Systems (MEMS) accelerometer. An industrial motor (Vexta) is used as an oriental reference. The STM microcontroller (MCU) has the role of memorizing the inclination sent from the motor with the corresponding acceleration into a Lookup Table (LUT) by using Flash memory. The full redundancy included dual accelerometers and MCUs to enhance the safety function for the operating system via two inclination channels. The support from the Low-pass filter and the zero-offset compensation for temperature change contribute to the measurement precision. For industrial applications, Control Area Network open (CANopen) is used as an embedded network communication system. Both static and dynamic cases were tested to verify the behavior of the inclination sensor. The designed structure provides high efficiency for inclinometer performance with accuracy $\pm 0.2^{o}$ and the stability is always guaranteed thanks to safety function. The designed inclinometer was used for a real excavator to verify its stability and operating performance. The project was carried out at the 'Sensor System' in Italy, an industrial company in the inclinometer field.**

***Index Terms*— MEMS, Industrial Inclinometer, Accelerometer, LUT, Redundancy, CANopen, Safety Function**

I. Introduction

INCLINOMETER plays a vital role in heavy industry, such as excavator, crane, or rotary drilling rig [1]. All these applications stand in need of the high precision and long-term stability of inclination measurement. Therefore, it is necessary to develop an inclinometer system with a robust orientation model and warning capability for the measurement error. The Microelectromechanical Systems (MEMS) has become popular in orientation calculation [4]–[6]. Among various types of MEMS sensors, the accelerometer [7]–[9] is considered as the primary key to detect the tilt angle by acceleration [1], [10]. The slope can be calculated by the fundamental formula, as described in [11], [12]. However, the traditional method of inclination measurement needs multiple mathematical steps of accelerometer calibration [13]–[19] and usually require re-calibration after being used for a specified period due to temperature change or external noise. Meanwhile, the industrial applications have demanded an inclinometer with an immediate operation, which is always ready to acquire inclination without further re-calibration, also in the case of a resetting sensor. Furthermore, the necessity of error warning has been emerged to guarantee positioning safety. Different from Inertial Navigation Systems [26], [27] by using the Inertial Measurement Unit [28], [29], the inclinometer is usually designed for heavy industry. At this time, an inclination sensor is installed to monitor the real-time tilt angle of the entire vehicle. For example, aerial work platforms need an inclination sensor to automatically brakes or alarms when the vehicle body is uneven or tilted to a certain angle. Also, for the excavator, the inclinometer supports the excavator to excavate at a construction site with a certain slope, which poses a severe test for the safety of their drivers and machinery. There are researches about the inclinometer system [2], [3]. They can achieve a good ability of slope tracking but the safety function, the guarantee of accurate performance during real operation were not mentioned. To guarantee the best operation of the sensor, a redundant inclinometer is an optimized solution that has a duplicate system with two nodes/channels of inclination data. Once the inclinometer has the problem, that fault could be noticed immediately based on the difference between angle data between 2 channels. There are numerous applications of inclinometer in the industry, so it is necessary to seek out a stable calibration and accurate orientation implementation for this sensor type.This paper presents an orientation structure to acquire a high performance of inclination. The inclinometer is calibrated based on the oriental motor as a reference, the accelerations and corresponding angles are memorized in Flash memory as Lookup Table (LUT) inside Microcontroller (MCU). The low pass filter and temperature compensation block are used to adjust the raw data to the proper value. In addition, the redundancy mode is designed as a safety enhancement that alerts the faults during the positioning process, as briefly illustrated in Fig. 1. Two nodes are on behalf of two channels, carried the inclination data from 2 accelerometers. The fault can be detected via the difference data between 2 nodes or can be called as two channels.

The content is organized as follows: Firstly, the low pass filter and temperature compensation algorithm are introduced. Secondly, the orientation calibration and inclinometer working principle is described, then the redundant system is presented. Thirdly, the experiment and data acquisition are analyzed in both static and dynamic cases. Finally, the designed inclinometer is tested in an excavator for 7 days to observe the operation

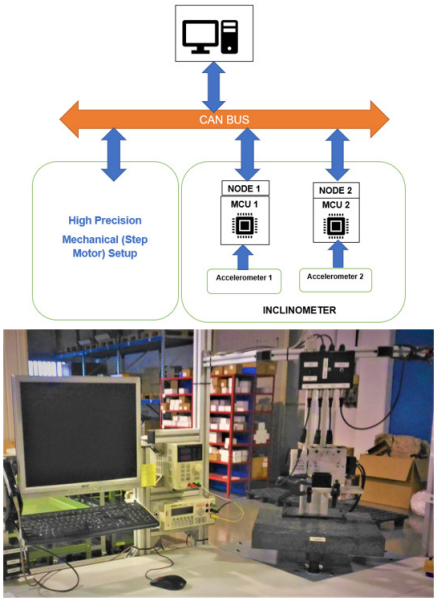

Fig. 1. Redundancy structure for orientation system and real mechanical setup

II. Low-pass filter and temperature compensation

A. Low-pass filter

A single-pole IIR (Infinite Impulse Response) filter is the effective filter for a digital accelerometer. This filter is a useful tool to remove high-frequency noise by allowing only low-frequency signals to pass through.

- Filter equation in z-transform:

$$H(z) = \frac{bz}{z-a} = \frac{b}{1-az^{-1}} \tag{1}$$

- Discrete-time signal of the input-output form:

$$y[n] = \alpha x[n] + by[n-1] \tag{2}$$

$$\alpha = e^{-2\pi\tau} \tag{3}$$

τ is the ratio, calculated by the desired corner frequency f_c and sample frequency f_s of the filter as described in [30]

$$\tau = \frac{f_c}{f_s} \tag{4}$$

Where: $x[n]$ is input, and $y[n]$ is the output signal. $\alpha + b = 1$ because of unity gain at DC in a filter. The acceleration data $Xacc$ and $Yacc$ enter the LP filter and go out as X_LP and Y_LP as shown in Fig.2

Fig. 2. Low-pass filter model

Fig. 3 shows the application for a sampling rate of 50 Hz, and the cut-off frequency is about 10 Hz.

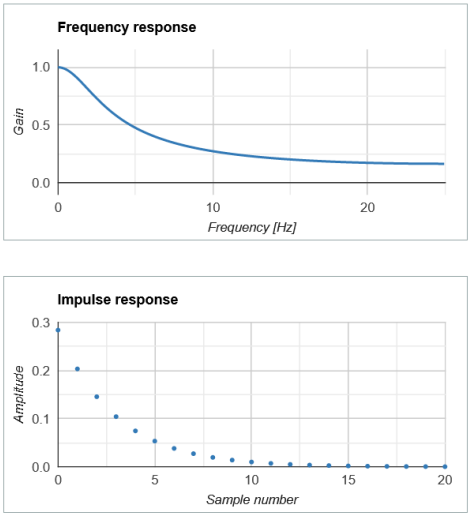

Fig. 3. Frequency response and impulse response

B. Temperature Compensation

Basically, the temperature change causes the variation of Zero-g offset like Fig. 4, so a simple but effective algorithm is used to adjust this value coherently. Usually, the accelerometer datasheet contains the coefficient of Zero-g offset change vs. temperature (TCO) in $mg/^oC$. The accelerometer offset temperature coefficient describes the deviation from the true value due to temperature changes from a nominal 25^oC condition. The offset variation is called a bias which is resulted from the product of TCO and temperature variation from 25^oC.

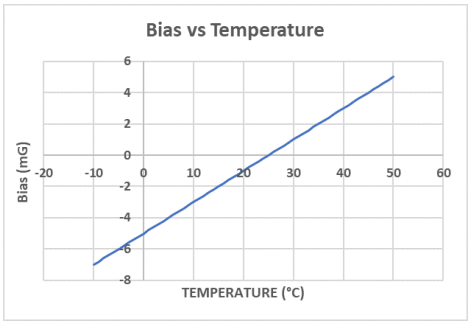

Fig. 4. Bias vs Temperature Chart

$$bias = TC0(T_{now} - 25) \tag{5}$$

Where T_{now} is the current temperature. modified In this way, the bias is always updated based on temperature variation to be removed from the raw acceleration.

For high accuracy of thermal calibration, the sensor circuit is calibrated by the climatic chamber as shown in Fig.5. The temperature adjustment was carried out to determine bias or characterization values for the platform.

- Procedures

Step1: The sensor circuit was put inside the climatic chamber.

Step2: The chamber is maintained at 25^oC for 10 minutes, then the acceleration value is set to 0.

Step 3: The chamber temperature is decreased to 0^oC for another 30 minutes. Next, the temperature is decreased to -10^oC. The offset values are recorded from each range.
Step 4: At this step, the temperature is adjusted from -10^oC to 70^oC with 10^oC steps. At each step, the temperature was kept stable for 40 minutes. The calibration results to determine new offsets, characterization values for the sensor circuit. To make modifications, the calibration process is repeated one more time to ensure the adjustments worked correctly. For each range, the bias is calculated with $mg/^oC$ and stored in system memory.

$$B_n = \frac{\Delta A}{\Delta T} = \frac{A_{Tn} - A_{Tn-1}}{T_n - T_{n-1}} \quad (6)$$

Where B_n is the bias at each adjustment step of temperature. T_n and T_{n-1} are the temperatures at the current step and the previous step. A_{Tn} and A_{Tn-1} are the calculated sensor error are the temperature at the current step and the previous step respectively. With this technique, the bias is appropriately removed from acceleration data.

Fig. 5. Climatic Chamber

III. LUT FILTER

Fig. 6 shows the direction of the accelerometer from the top of view in this project. The LUT method imports the angle of inclination and its corresponding acceleration. After calibration, each time the sensor reaches the sensing acceleration of the X or Y-axis, it will provide the corresponding oriental angle of roll or pitch based on the LUT data. In this method, the acquisition values from Z-axis are ignored, the LUT filter only memorizes the acceleration from X and Y axis independently.

The method requires an accurate reference for the calibration. Therefore, an oriental motor for the industry is selected and verified by protractor 360^o to assure its precision which is popularly applied to Inertial measuring units (IMU) [21].

- Calibration process:

The technique procedures are shown in Fig. 7 and Fig. 8. The inclinometer is mounted on the stepper motor. The Motor rotates at a specified resolution of step. During motor rotation, the MCU memorizes the angel and correlative acceleration

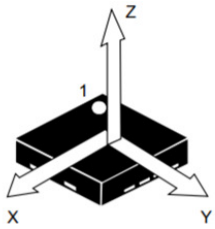

Fig. 6. (Top view) direction of the detectable accelerations [20]

value after a low pass filter. Roll and pitch data are calibrated separately then stored in 2 independent tables. In this way, the LUT filter contains all the calibration values.

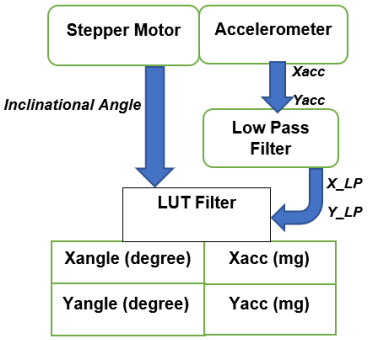

Fig. 7. Calibration setup of inclinometer

- Operating Process

After the calibration part, the tilt will be detected via acceleration values. The accelerometer sends the acquisition data to a low pass filter, and then the data are compensated with the temperature change before entering to LUT filter. Finally, the inclination angle is accomplished according to the memorized table.

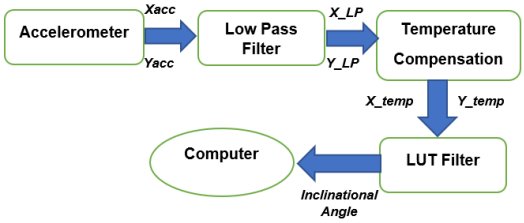

Fig. 8. Operating Process of inclinometer

Where: $Xacc, Yacc$ are the accelerometer acquisition on X-axis and Y-axis, respectively. X_ LP, Y_ LP are the filtered value from X-axis and Y-axis, respectively, after Low Pass Filter. X_temp, Y_ temp are the outputs of temperature compensation. Inclinational Angle is the tilt of the X-axis and Y-axis, with respect to the Earth frame.

- Data linearization

When the acquisition value falls between 2 memorized data, the firmware includes an algorithm to calculate the gap between real data and two acceleration points before and after, then equalizes the measured data with the closest point as demonstrated in Fig. 9. The distance between 2 consecutive

acceleration X_{n-1} and X_n is computed to seek the middle point between them. I_{n-1} and In are two corresponding inclination of X_{n-1} and X_n respectively. The lowest resolution of inclinator is 0.001^o.

$$\Delta X = \frac{X_n - X_{n-1}}{2} \tag{7}$$

- If $|X\_LP| < |X_{n-1} + \Delta X/2| \Rightarrow Inclination = I_{n-1}$
- If $|X\_LP| > |X_{n-1} + \Delta X/2| \Rightarrow Inclination = I_n$

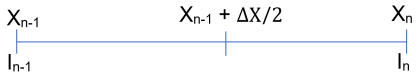

Fig. 9. Two consecutive points in LUT

- The architecture of system flash memory

The calibration data are stored into flash memory of MCU-STM32 from address 0x0800 0000 to 0x0801 FFFF as shown in Fig. 10. Here, the Cyclic Redundancy Check (CRC) has the mission to verify data transmission or storage integrity. In addition, CRC computes the signature of the application software during run-time, to be compared with a reference signature generated at link-time and stored at a given memory location. Bootloader manages the erase operation of this location before writing in a Data memory location. Data on temperature calibration and accelerations with coherent inclinations are stored in flash. This technique guarantees the long-term performance of the sensor.

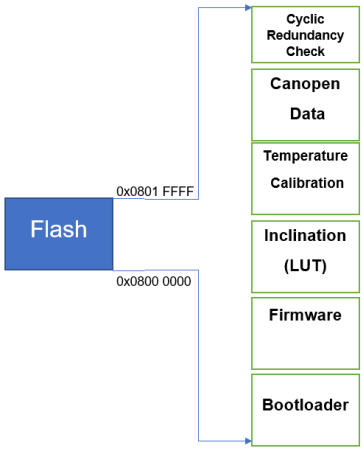

Fig. 10. Stored data architecture in flash

IV. Redundant Function

A. Redundancy Architecture

Faults in position measurement pose a severe hazard during dynamic positioning [22]. Therefore, the redundancy plays a critical role in the inclinometer safety. Dual accelerometers transmit the data which are used for the inclination measurements then sent out via two nodes. At this point, two channels provide oriental angles as illustrated in Fig. 11 . To guarantee the safety of the system, the difference between 2 orientation angles from 2 nodes (Δ angle) cannot exceed a working threshold (Δth). Otherwise, the error message will be sent to the user. The redundant mode must guarantee stable performance from both 2 sensor channels based on Δth. Under the same operating condition, 2 angles values supposed to be the same or close to each other.

- If Δ angle exaggerates Δth frequently, it indicates the less accuracy of the inclinometer at that period and the acquisition data is trust-less.
- Without redundant mode, it is difficult for the user to realize whether the inclinometer is working properly or not.

The Δth is selected with value 0.40^o. The tolerance error of each inclinometer channel is 0.20^o. Here, we take into account that when both two sensor channels get the maximum error. One node has less value than the reference 0.20^o; another node exceeds value than the reference 0.20^o. In this case, the difference between them is 0.40^o.

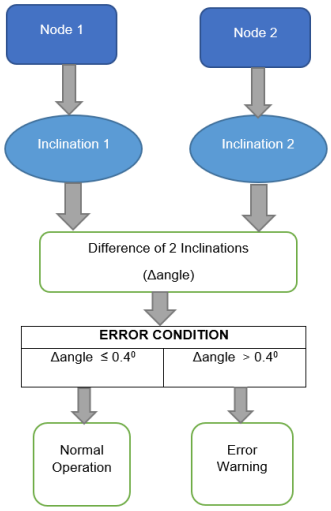

Fig. 11. Redundancy chart

B. Error Solutions

When the positioning warning frequently occurs more than 110 times for 10 minutes, the priority solution is to stop the sensor motion for 45 seconds as demonstrated in Fig. 12 . Perhaps, the data from one node arrives in delay. After the waiting period, if the inclination difference from 2 nodes come back to lower than 0.40^o, it means that the problem is solved. Otherwise, the power supply should be checked, and the inclinometer supposed to be reset. They are two fundamental errors that can be identified easily by a redundant function as described in Tab. I.

V. Experimental Setup

In the experiment, a robust setup is constructed accurately for the calibration as well as the acquisition of the proposed inclinometer as shown in Fig. 13. The sensors involved in acquiring data for the experiments are the accelerometer LIS2DW12 [20] with the Output Data Rate of 50 Hz. This

TABLE I
ERROR WARNING

Error type	Solution
Data Delay	Stop the sensor motion for 45 seconds (s) ⇒ System comes back to work normally.
Error of physical material (power supply problem)	Checking power supply-Reset the system.

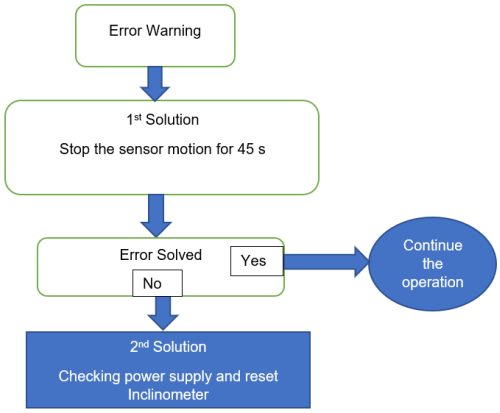

Fig. 12. Error and Solutions

device is a system-in-package featuring a tri-axial digital linear acceleration sensor with a 16-bit resolution and selectable full-range scale ± 2 to ± 16 g full scale. The NUCLEO-F103RB [23] with a maximum clock frequency of 72 MHz is used to implement the LUT filter into an external MCU STM32F103C8T6 [24] via ARM's Serial Wire Debug (SWD). This MCU with Flash Memory of 64 kB is embedded in the inclinometer. The sensor is interfaced to the MCU development via a Serial Peripheral Interface (SPI) communication line in full-duplex mode. The Controller Area Network open (CANopen bus) is used as communication protocol and device profile specification for the embedded network. High precision and robust stepper motor: Vexta oriental motor DGM130R-ASAA [25] used as a reference that rotates 1 $degree$ each 1500 ms. A metal piece is designed to handle the inclinometer appropriately, which is mounted on the stepper motor for left-right rotation.

The LUT algorithm is programmed into the inclinometer. After sending a message to activate, the microcontroller starts memorizing the X-axis for roll and Y-axis for pitch. In this way, the stepper motor motion and the LUT memorization are carried out simultaneously. At this point, the inclinometer will measure the inclinational angles corresponding to the value of the X and Y-axis in LUT. The cover of the inclinometer is made up of metallic to resist the vibration by its weight. After the calibrating process, the setup will go around in a circle again to verify the performance of the calibrated inclinometer. The maximum toleration is only allowed at 0.20^o. In the case the error evaluation exaggerates this tolerance, the inclinometer must be re-calibrated. In the experiment, the inclinometer

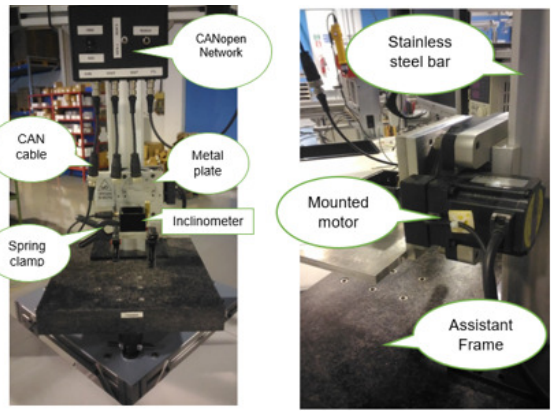

Fig. 13. Inclinometer setup and mounted motor on setup

is applied in the range from -90^o to 90^o.

VI. EXPERIMENTAL RESULTS

Both static and dynamic tests were carried out to inspect the stability and precision of the redundant inclinometer. All the errors were reported in absolute value for simple observation and analysis, based on the reference angle of the motor.

A. Static Test

For the static test, the motor is rotated step by step from -90^o to 90^o. with a differential step of 10^o to verify the acquisition values from 2 nodes. This test includes 2 parts: the 1st part verifies the performance of the inclinometer by error calculation between the acquired angle and reference angle. The maximum tolerance error is 0.20^o. In the 2nd part, the difference between 2 nodes calculated during the rotation process for safety function.

- Performance

In this part, the measured angle of the X-axis and Y-axis are verified by comparing it with the reference value, as shown in Fig. 14 and Fig. 15. The designed inclinometer operates appropriately with small errors on both axes under the tolerance range of 0.20^o. Generally, the errors are higher when the angle is closer to 90^o. As far away from the Earth frame, it is more challenging to attain an accurate angle.

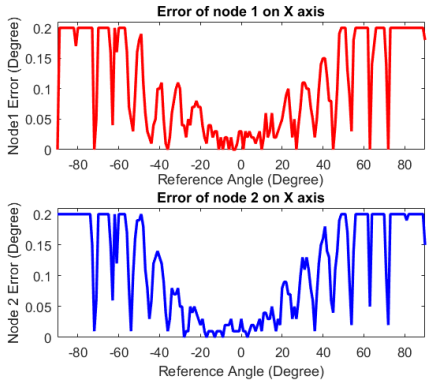

Fig. 14. . Error of angle acquisition on X-axis

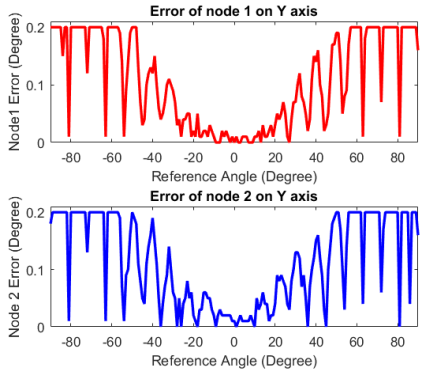

Fig. 15. Error of angle acquisition on Y-axis

TABLE II
ERROR MEASUREMENT OF STATIC TEST

Axis	RMSE of Node 1 (deg)	RMSE of Node 2 (deg)	Mean of 2 Nodes difference (deg)	Error Warning
X	0.106	0.111	0.018	No
Y	0.107	0.112	0.015	No

- Difference between 2 nodes

At each acquired angle, the difference between 2 nodes is calculated. By that way, the Δ angle is collected or can be called as error between 2 nodes. This maximum Δ angle reached at -90^o on X-axis and at close to 90^o on Y-axis like Fig. 16. At this point, the synchronization between 2 nodes is very stable.

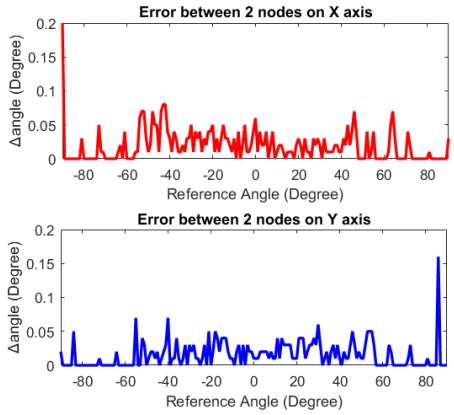

Fig. 16. Difference value between 2 nodes on X-axis and Y-axis

Root-mean-square-error (RMSE) of inclination acquisition, reported in Tab. II to analyze the accuracy from 2 channels of the sensor in degree (deg). The mean value of the difference between 2 nodes is calculated to guarantee the safety function of the system. The RMSE of 2 nodes is small, with a little difference between them.

B. Dynamic Test

For stability examination, the setup is set at rotation speed of 80 degrees/second from -40^o to 40^o. About 10 repetitive cycles are processed on X-axis and Y-axis as shown in Fig.17 and Fig. 18. The data of the inclinometer appropriately follow the trend of the dynamic rotation with high accuracy.

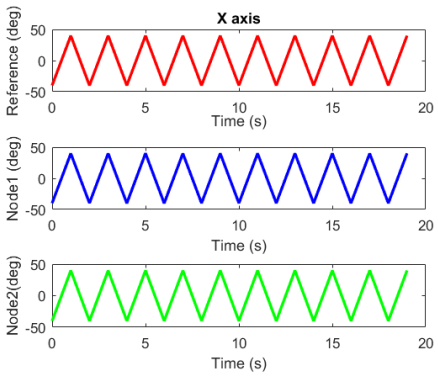

Fig. 17. Dynamic Positioning on X-axis

The data from Tab. III confirm the certainty and stability of the inclinometer by the RMSE no more than 0.10. There is no error warning, thanks to the precise performance. The maximum difference value between 2 nodes is 0.20^o, so the system is always in normal operating condition.

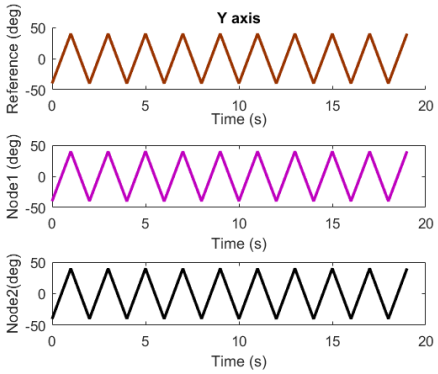

Fig. 18. Dynamic Positioning on Y-axis

TABLE III
ERROR MEASUREMENT OF DYNAMIC TEST

Axis	RMSE of Node 1 (deg)	RMSE of Node 2 (deg)	Mean of 2 Nodes difference (deg)	Error Warning
X	0.091	0.100	0.2	No
Y	0.088	0.085	0.1	No

VII. FAULT DETECTION ON REAL APPLICATION

For 7 days, the designed inclinometer was tested in an excavator as support of excavation depth measurement control via the pitch angle (angle on Y-axis) of the mechanical arm. Fig. 19 indicates the position of the testing sensor. Each day the sensor was in work for 3 hours, with 50 samples are extracted per second. Fig. 20 reports the number of detected errors per day. The inclinometer works well as the expectation. No error occurred except day 5 where the power supply was unstable because of a technical problem. Consequently, a fault detected thanks to the safety function between 2 nodes on Y-axis. Each node considered as a channel.

Fig. 19. Testing Inclinometer in Excavator

Fig. 21 shows the maximum of angle variation between 2 nodes, approximately 10. The different measurements between 2 nodes is called as delta channel. In the fault case, the delta channel still can be a standard (less than 0.20^o), but only for a short period then rise. This signal indicates that the system is in an unstable situation, and the users need to check the operating system to guarantee stability. The delta channel frequently surpass 0.40^o for 10 minutes. In this way, error detected, and the inclinometer was temporarily stopped and reset. After this period, the sensor comes back to work normally

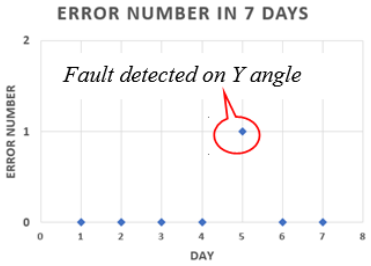

Fig. 20. Error number for 7 days

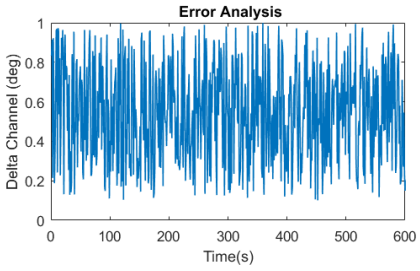

Fig. 21. Variation of delta channel on X-axis

VIII. CONCLUSION

A highly effective system for inclinometer was designed with a successful operation in both static and dynamic cases. The redundant mode guarantees the safety of oriental operation which is always ready to alert the users in the case of risk accuracy. As reported results in Tab. II and Tab. III, the redundant mode does not detect any error during the experiment, showed the robust and potent design of the inclinometer. In the real application with the excavator, the fault was detected thanks to the proposed safety function to resolve the technical problem. The proposed structure of the inclinometer is strongly recommended for the application in heavy industry with a practical method of orientation and long-term stability.

REFERENCES

[1] G. Qinglei, L. Huawei, M. Shifu and H. Jian, "Design of a Plane Inclinometer Based on MEMS Accelerometer," *International Conference on Information Acquisition, Seogwipo-si*, 2007, pp. 320-323.

[2] J. Wang, G. Gao and P. Liu, "The study on lange-angle CANBUS 2-axis inclinometer of rotary drilling rig," *2nd IEEE International Conference on Information Management and Engineering*, Chengdu, 2010, pp. 95-97.

[3] L. Da-wei and G. Tao, "Design of Dual-axis Inclinometer Based on MEMS Accelerometer," *Third International Conference on Measuring Technology and Mechatronics Automation*, Shangshai, 2011, pp. 959-961.

[4] A. Harindranath and M. Arora, "MEMS IMU Sensor Orientation Algorithms-Comparison in a Simulation Environment," 2018 International Conference on Networking, Embedded and Wireless Systems (ICNEWS), Bangalore, India, 2018, pp. 1-6.

[5] S. Hosseinyalamdary, Y. Balazadegan, C. Toth, "Tracking 3D Moving Objects Based on GPS/IMU Navigation Solution Laser Scanner Point Cloud and GIS Data", ISPRS Int. J. Geo-Inf., vol. 4, pp. 1301-1316, 2015.

[6] M. L. Hoang, S. D. Iacono, V. Paciello and A. Pietrosanto, "Measurement Optimization for Orientation Tracking based on No Motion No Integration Technique," *IEEE Transactions on Instrumentation and Measurement*, doi: 10.1109/TIM.2020.3035571.

[7] X. Zou, P. Thiruvenkatanathan and A. A. Seshia, "A Seismic-Grade Resonant MEMS Accelerometer," *Journal of Microelectromechanical Systems*, 3rd vol. 23, no. 4, pp. 768-770, Aug. 2014.

[8] M. Bodnicki and S. Łuczak, "Comments on "Delay Compensation of Tilt Sensors Based on MEMS Accelerometer Using Data Fusion Technique"," *in IEEE Sensors Journal*, , vol. 18, no. 3, pp. 1333-1335, 1 Feb.1, 2018.

[9] S. A. Zotov, B. R. Simon, A. A. Trusov and A. M. Shkel, "High Quality Factor Resonant MEMS Accelerometer With Continuous Thermal Compensation," *IEEE Sensors Journal*, vol. 15, no. 9, pp. 5045-5052, Sept. 2015.

[10] M. L. Hoang, M. Carratù, and V. Pacielloand A. Pietrosanto, "A new orientation method for inclinometer based on mems accelerometer used in industry 4.0", *IEEE 18th International Conference on Industrial Informatics (INDIN 2020)* , 2020.

[11] P. Promrit, S. Chokchaitam and M. Ikura, "In-Vehicle MEMS IMU Calibration Using Accelerometer," *IEEE 5th International Conference on Smart Instrumentation, Measurement and Application (ICSIMA)*, Songkla, Thailand, 2018, pp. 1-3.

[12] L. Cocco and S. Rapuano, "Accurate Speed Measurement Methodologies for Formula One Cars," *IEEE Instrumentation and Measurement Technology Conference IMTC*, Warsaw, 2007, pp. 1-6.

[13] X. Lu and Z. Liu, "IEKF-based Self-Calibration Algorithm for Triaxial Accelerometer," *3rd International Conference on Information Science and Control Engineering (ICISCE)*, Beijing, 2016, pp. 983-987.

[14] Z. Chen, H. Li, X. Du and J. Yan, "Research on the Calibration Method of MEMS Accelerometer Based on Recursive Least Squares," *IEEE International Conference on Mechatronics and Automation (ICMA)*, Changchun, 2018, pp. 533-538.

[15] P. Schopp, H. Graf, W. Burgard and Y. Manoli, "Self-Calibration of Accelerometer Arrays," *IEEE Transactions on Instrumentation and Measurement*, vol. 65, no. 8, pp. 1913-1925, Aug. 2016.

[16] J. Chang, J. Cieslak, A. Zolghadri, J. Dávila and J. Zhou, "Design of sliding mode observers for quadrotor pitch/roll angle estimation via IMU measurements," 2015 Workshop on Research, Education and Development of Unmanned Aerial Systems (RED-UAS), Cancun, 2015, pp. 393-400.
[17] Zhiwen Liu, Xiaoming Zhang, Xihong Ma, Two-Step Calibration Method Based on the MIMU Measurement System, Micronanoelectronic Technology, 54(02): 113–119, 2017.
[18] Haiyin Zhang, Boxian He, Tieshan Zhen, Yi Wu, Triaxial Accelerometer Error Compensation Method Based on Ellipsoid Fitting, Sensor World, 21(06): 7–10, 2015.
[19] Jie Li, Xiaochun Tian, Yubao Fan, Jun Liu, Field Fast Calibration Techniques for Missile-Borne MIMU Based on Ellipsoid Fitting, Journal of Projectiles, Rockets, Missiles and Guidance, 33(01): 10–12, 2013.
[20] STMicroelectronics, LIS2DW12 MEMS digital output motion sensor: high-performance ultra-low-power 3-axis "femto" accelerometer, July 2019.
[21] Lukáš Palkovič, Jozef Rodina, Ľuboš Chovanec, Peter Hubinský, "Integration of Inertial Measuring Unit Platform into MATLAB Simulink, 9th IFAC Symposium Advances in Control Education, Volume 45, Issue 11, Russia, June 19-21, 2012. M. Young, The Technical Writer's Handbook. Mill Valley, CA: University Science, 1989.
[22] R. H. Rogne, T. A. Johansen and T. I. Fossen, "Observer and IMU-based detection and isolation of faults in position reference systems and gyrocompasses with dual redundancy in dynamic positioning," *2014 IEEE Conference on Control Applications (CCA)*, Juan Les Antibes, 2014, pp. 83-88.
[23] STMicroelectronics, STM32 Nucleo-64 boards - Product Specifications, April 2019.
[24] STMicroelectronics, STM32F103xB,Medium-density performance line ARM®-based 32-bit MCU with 64 or 128 KB Flash, USB, CAN, 7 timers, 2 ADCs, 9 com. interfaces, August 2015.
[25] ORIENTAL MOTOR CO., LTD "Hollow Rotary Actuators DG Series DG85, DG130, DG200", 2011
[26] M. Malleswaran, S. A. Deborah, S. Manjula and V. Vaidehi, "Integration of INS and GPS using radial basis function neural networks for vehicular navigation," *11th International Conference on Control Automation Robotics and Vision, Singapore*, 2010, pp. 2427-2430, doi: 10.1109/ICARCV.2010.5707295.
[27] H. Hamidi, E. S. Abdolkarimi and M. R. Mosavi, "Prediction of MEMS-based INS Error Using Interval Type-2 Fuzzy Logic System in INS/GPS Integration," *25th International Computer Conference, Computer Society of Iran (CSICC)*, Tehran, Iran, 2020, pp. 1-5, doi: 10.1109/CSICC49403.2020.9050081.
[28] M. L. Hoang, A. Pietrosanto, S. D. Iacono and V. Paciello, "Pre-Processing Technique for Compass-less Madgwick in Heading Estimation for Industry 4.0," *IEEE International Instrumentation and Measurement Technology Conference (I2MTC)*, Dubrovnik, Croatia, 2020, pp. 1-6, doi: 10.1109/I2MTC43012.2020.9128969.
[29] M. Carratù, S. D. Iacono, M. Long Hoang and A. Pietrosanto, "Energy characterization of attitude algorithms," *IEEE 17th International Conference on Industrial Informatics (INDIN)*, Helsinki, Finland, 2019, pp. 1585-1590, doi: 10.1109/INDIN41052.2019.8972300.
[30] L. Cao, "Practical Issues in Implementing a Single-Pole Low-Pass IIR Filter [Applications Corner]," *IEEE Signal Processing Magazine*, vol. 27, no. 6, pp. 114-117, Nov. 2010, doi: 10.1109/MSP.2010.938097.